Element-Resolved Thermodynamics of Magnetocaloric LaFe$_{13-x}$Si$_x$

M. E. Gruner,[1,2,*] W. Keune,[1,3] B. Roldan Cuenya,[4] C. Weis,[1] J. Landers,[1] S. I. Makarov,[1,3] D. Klar,[1]
M. Y. Hu,[5] E. E. Alp,[5] J. Zhao,[5] M. Krautz,[2] O. Gutfleisch,[6] and H. Wende[1]

[1]*Faculty of Physics and Center for Nanointegration Duisburg-Essen (CENIDE), University of Duisburg-Essen,
47048 Duisburg, Germany*
[2]*IFW Dresden P.O. Box 270116, 01171 Dresden, Germany*
[3]*Max Planck Institute of Microstructure Physics, 06120 Halle, Germany*
[4]*Department of Physics, Ruhr-University Bochum, 44780 Bochum, Germany*
[5]*Advanced Photon Source, Argonne National Laboratory, Argonne, Illinois 60439, USA*
[6]*Materials Science, TU Darmstadt, 64287 Darmstadt, Germany*
(Received 19 August 2014; published 4 February 2015)

By combination of two independent approaches, nuclear resonant inelastic x-ray scattering and first-principles calculations in the framework of density functional theory, we demonstrate significant changes in the element-resolved vibrational density of states across the first-order transition from the ferromagnetic low temperature to the paramagnetic high temperature phase of LaFe$_{13-x}$Si$_x$. These changes originate from the itinerant electron metamagnetism associated with Fe and lead to a pronounced magneto-elastic softening despite the large volume decrease at the transition. The increase in lattice entropy associated with the Fe subsystem is significant and contributes cooperatively with the magnetic and electronic entropy changes to the excellent magneto- and barocaloric properties.

Ferroic materials allow for significant adiabatic temperature changes induced by realistic electrical and magnetic fields, by external stress and under pressure [1–4]. This allows their use in solid-state refrigeration concepts as an energy efficient alternative to the classical gas-compressor scheme. A good cooling material is characterized by a large isothermal entropy change $|\Delta S_{\mathrm{iso}}|$, which determines the latent heat to be taken up during a first-order transformation in conjunction with a high adiabatic temperature change $|\Delta T_{\mathrm{ad}}|$. Apart from the prototype Gd-based systems [5], a large number of suitable materials were proposed, which undergo a magnetic first-order transition and perform well in both respects (see, e.g., Ref. [6]). Among the outstanding materials are LaFe$_{13-x}$Si$_x$-based systems ($1.0 \leq x \leq 1.6$) [7–9], which consist of largely abundant components [3]. Their structure corresponds to cubic NaZn$_{13}$ ($Fm\bar{3}c$, 112 atoms in the unit cell), with two distinguished crystallographic Fe sites, Fe$_\mathrm{I}$ and Fe$_\mathrm{II}$, on the eightfold ($8b$) and 96-fold ($96i$) Wyckoff positions, respectively. La resides on ($8a$) sites, while Si shares the ($96i$) site with Fe$_\mathrm{II}$ [10–12]. The Curie temperature T_C of the ferromagnetic (FM) to paramagnetic (PM) transformation is around 200 K, depending on composition. T_C increases proportionally with increasing Si content [13,14], but the transition changes to second order, while $|\Delta S_{\mathrm{iso}}|$ and $|\Delta T_{\mathrm{ad}}|$ decrease significantly. By concomitant hydrogenation and Mn substitution, T_C can be precisely adjusted to ambient conditions without severe degradation of the caloric performance [15–18]. The first-order magnetic transformation is accompanied by an abrupt isostructural volume decrease of 1% for $x = 1.5$ upon the loss of magnetic order [19].

This also gives rise to a large *inverse* barocaloric effect [20]. In the FM phase the thermal expansion coefficient is largely reduced or even negative [10,21], which presents similarities with the Invar-type thermal expansion anomalies discovered in Fe$_{65}$Ni$_{35}$ (and other ferrous alloys) more than 100 years ago (see, e.g., Ref. [22]).

Consequently, the moment-volume instability of La-Fe-Si has been discussed in terms of the itinerant electron metamagnetism (IEM) arising from the (partially) nonlocalized character of the Fe moments [23,24] within a phenomenological Ginzburg-Landau description [25,26]. The IEM picture gained further support from first-principles calculations [27–29] through the identification of metastable minima of the binding surface, which correspond to metastable magnetic configurations at distinct volumes. This is also a characteristic feature of Fe-Ni Invar, where the compensation of thermal expansion is linked to the redistribution of charge between nonbonding majority spin states above and antibonding minority spin states below the Fermi level [30]. However, further *ab initio* work on La-Fe-Si concentrates on the electronic structure in the FM phase and the non-spin-polarized state [25,31–33], while thorough characterization of the paramagnetic phase is still missing.

In this Letter we will establish the link between the electronic structure of La-Fe-Si and its macroscopic thermodynamic behavior in both the FM and the PM phase, by a combination of nuclear resonant inelastic x-ray scattering (NRIXS) and *ab initio* lattice dynamics. We demonstrate for the first time that temperature-induced magnetic disorder causes distinct modifications in the vibrational density of states (VDOS) of a cubic metal.

We disentangle the elemental contributions to the VDOS, which determines the intrinsic vibrational thermodynamic properties, such as lattice entropy, and relate them to phase-induced changes in the electronic structure.

The isothermal entropy change is usually divided up as $\Delta S_{iso} = \Delta S_{mag} + \Delta S_{lat} + \Delta S_{el}$, i.e., into the contributions from the magnetic, lattice, and electronic degrees of freedom, respectively [1]. These are associated with the configuration entropy arising from spin disorder, excitation of quasiharmonic phonons, and thermal occupation changes of the electronic states, respectively. Mixed interactions are often not taken into account separately, although they might enhance ΔS_{iso} significantly [34] and can be expected for $3d$ metals [1]. Anharmonic contributions are neglected here as well. For La-Fe-Si, ΔS_{mag} is expected to be the driving contribution, while ΔS_{el} is considered negligible and ΔS_{lat} is deemed to counteract assuming a quasiharmonic renormalization of the Debye temperature Θ [14,35]. In the following we will demonstrate that both ΔS_{lat} and ΔS_{el} contribute *cooperatively* to the magneto-caloric effect. The sign of ΔS_{lat} is determined by the IEM of Fe, which affects magneto-elastic interactions and thus modifies phonon frequencies oppositely to what is expected from Grüneisen theory.

For the measurements, we used a polycrystalline sample with nominal composition $LaFe_{11.6}Si_{1.4}$ (Fe with 10% enrichment in ^{57}Fe); for details, see Ref. [36]. The sample was characterized by x-ray diffraction and 14.4-keV Mössbauer backscattering spectroscopy [36], showing that $89 \pm 1\%$ of the Fe atoms in the sample are in the $La(Fe, Si)_{13}$ phase and $11 \pm 1\%$ are in the bcc Fe secondary phase [9,18]. Magnetization measurements reveal (in agreement with Ref. [7]) a first-order FM-PM transition at $T_C = 189$ K with a hysteresis of 3 K. NRIXS [65–67] was performed at the Sector-3 beam line at the Advanced Photon Source, Argonne National Laboratory. The incident x-ray energy was around $E_0 = 14.412$ keV, the nuclear resonance energy of ^{57}Fe. The x-ray beam is highly monochromatized with an energy bandwidth of 1 meV [68]. NRIXS was carried out in zero external magnetic field at four different measurement temperatures T_{exp}, two in the FM phase (62 K, 164 K) and two in the PM phase (220 K, 299 K). The ^{57}Fe-specific VDOS were extracted from the NRIXS data using the PHOENIX program [69] and corrected for the α-Fe contribution [36].

The *ab initio* part is carried out with the VASP package [70,71] in the framework of density functional theory (DFT) using the generalized gradient approximation [72]. We represented the 112 atom unit cell by a 28 atom primitive cell with fcc basis and introduced three Si atoms on the (96*i*) sites, i.e., $x = 1.5$ Si per formula unit (f.u.), such that the space group is minimally reduced to rhombohedral ($R3$) with still 12 inequivalent lattice sites. For the PM phase, we carefully determined a stable collinear spin arrangement with 10 inverted Fe moments, which has a

total spin magnetization of 3.75 μ_B/f.u. compared to 24.5, μ_B/f.u. for FM. An average spin moment of 1.7 μ_B/Fe was obtained for PM as compared to 2.2 μ_B/Fe for FM, in good agreement with available Mössbauer, neutron diffraction, and DFT data [12,13,28,73]. We optimized ionic positions and volume before the dynamical matrix was constructed with Alfè's PHON code [74] based on the Hellmann-Feynman forces obtained from 56 $\pm$ displacements in a $2 \times 2 \times 2$ supercell. This yields the VDOS, $g(E)$, from which we obtain thermodynamic quantities such as the lattice entropy S_{lat} and their temperature dependence [75,76]. We estimate the lattice entropy in the harmonic approximation using the equilibrium volume of both magnetic states since thermal expansion is small or absent below and immediately above T_C. For further details, see Ref. [36].

We observe striking differences in the experimental Fe-projected VDOS below and above T_C (Fig. 1), in particular, the disappearance of the distinct phonon peak near 28 meV (arrows) in the PM state. This unusual 17% effect (see α-Fe in Ref. [77]) is a distinct manifestation of the impact of magnetic disorder on both the low- and high-energy parts of the phonon spectra which is known from iron oxide [78] but has not been demonstrated this clearly
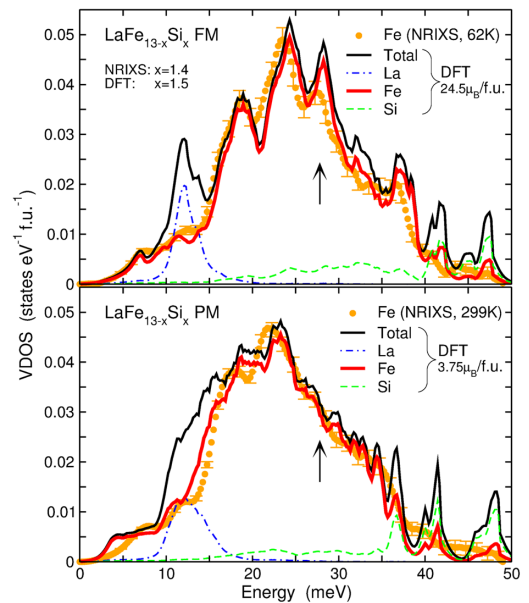

FIG. 1 (color online).　Element-resolved VDOS of FM and PM $LaFe_{13−x}Si_x$. Orange circles with error bars denote the partial ^{57}Fe DOS obtained with NRIXS at $T_{exp} = 62$ K and $T_{exp} = 299$ K, respectively, corrected for the bcc Fe secondary phase contribution [36]. The lines refer to the DFT results for different magnetizations ($M = 24.5$ μ_B/f.u. and $M = 3.75$ μ_B/f.u., respectively). The thick red lines denote the partial DOS of the Fe atoms, which compares to the NRIXS measurement. The thinner black lines, the green dotted lines, and the blue dash-dotted lines refer to the total VDOS and the partial contributions of Si and La, respectively. The arrows indicate the position of the phonon peak near 28 meV in the FM phase, which disappears in the PM phase.

for a metallic system. DFT reproduces all relevant features of the partial VDOS of Fe obtained with NRIXS, including the uniform shift to lower energies above T_C, which verifies our La and Si partial and the total VDOS, which we can only obtain from DFT. Thus, we encounter an overall softening in $g(E)$ upon heating, which overrides the stiffening expected from Grüneisen theory, according to the volume contraction. From the NRIXS $g(E)$ we obtain the temperature-dependent lattice entropy $S_{lat}(M_{exp}, V_{exp})$ corresponding to volume V and magnetization M at the respective T_{exp} using the well-known textbook relation [76] neglecting the T dependence of M. Figure 2 shows that changing from FM to PM configurations results in an increase in S_{lat} at T_C, which amounts to $\Delta S_{lat}^{Fe}|_{T_C} = 11$ Jkg^{-1} K$^{-1} = 0.10 k_B$/Fe calculated from the NRIXS VDOS for $T_{exp} = 62$ and 299 K. This is about one-half of $\Delta S_{iso} = 24$ Jkg^{-1} K^{-1} from literature [7], obtained from integrating specific heat across the field-induced transition. From our NRIXS data closer to T_C ($T_{exp} = 164$ and 220 K), we obtain a reduced $\Delta S_{lat}^{Fe}|_{T_C} = 5$ Jkg^{-1} K^{-1}. As thermal expansion is largely canceled, the difference of 6 Jkg^{-1} K^{-1} originates from the increasing spin disorder in the FM phase and the remaining spin correlation in the PM phase and is therefore another manifestation of the strong magnetoelastic coupling in La-Fe-Si, arising from the observed changes in the VDOS, $g(E)$, across the phase transition. The entropy Debye temperature Θ_S, derived from the logarithmic moment of the partial Fe NRIXS $g(E)$ [75,79,80], decreases by 3% from $\Theta_{62\ K}^{Fe} = 371$ K (FM) to $\Theta_{299\ K}^{Fe} = 360$ K (PM), whereas normal Grüneisen behavior

would rather result in a 1%–2% increase due to the large negative volume change at T_C. The DFT model fully confirms this trend and yields an even larger $\Delta S_{lat}^{tot}|_{T_C} = 32$ Jkg^{-1} K^{-1} from the total $g(E)$, which coincides with the computed partial Fe contribution. The elemental decomposition of ΔS_{lat} in Fig. 3 (left) shows some spread according to the chemical and electronic configuration, which also have a strong influence on the interatomic spacings [12,73,81], in particular, for the Fe sites, which encounter a change in magnetic order. Here, the average contribution (thick line) is large and positive, while for La and Si it is vanishing or even slightly negative. Since symmetry does not change, the anomalous sign of ΔS_{lat} is thus solely related to the change of the magnetic environment of the Fe atoms.

This trend can be explained through adiabatic electron phonon coupling, which has recently been identified as the cause of anomalous softening or stiffening in several Fe-based materials [82–84] upon temperature-dependent positional and chemical disorder. Such disorder broadens minima or maxima in the electronic DOS, $D(E)$, around E_F, where a high availability of electronic states assists the screening of perturbations from a displaced atom. Indeed, we can identify a likewise correlation between the PM and FM phase in the site-resolved lattice entropy changes $\Delta S_{lat,i}$ and in the site-resolved DOS $\Delta D_i(E_F)$ of the respective site i. This trend is particularly pronounced for the minority electrons corresponding to the respective site (Fig. 3, right) and originates from the IEM of Fe, as shown by the electronic DOS. The FM DOS in the upper panel of Fig. 4 exhibits a completely filled majority d channel and a nearly half filled minority channel [25,31–33]. The large exchange splitting moves the mid-d-band minimum found in the majority channel at -2 eV right to the Fermi level E_F in the minority channel, which is a stabilizing feature for
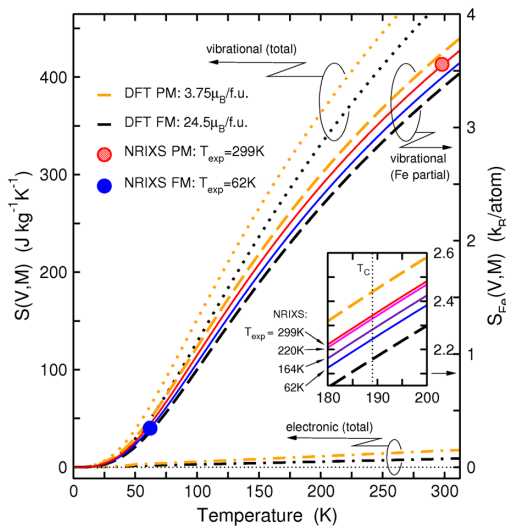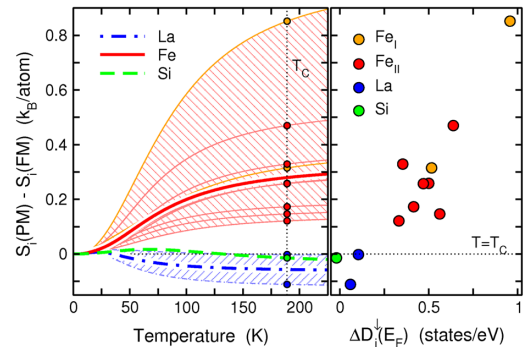

FIG. 2 (color online). Total (left scale) and Fe contribution (right scale and inset) to the lattice entropy and electronic entropy of the FM and PM phases. For a Si content of $x = 1.5$ (DFT) both scales are equivalent. The lines are calculated from $g(E)$ for the volume V and magnetization M corresponding to the measurement temperature T_{exp} (circles) or $T = 0$ (DFT), respectively.

FIG. 3 (color online). Element- and site-resolved difference in lattice entropy $\Delta S_{lat,i} = S_{lat,i}(PM) - S_{lat,i}(FM)$ from DFT (left-hand side). The thick lines refer to the elemental averages, thin lines refer to values for the inequivalent lattice sites i. The right-hand graph demonstrates the correlation between the site-resolved $\Delta S_{lat,i}$ at T_C and the change in the site-resolved minority spin DOS at E_F, $\Delta D_i^{\downarrow}(E_F) = D_i^{\downarrow}(E_F, PM) - D_i^{\downarrow}(E_F, FM)$.
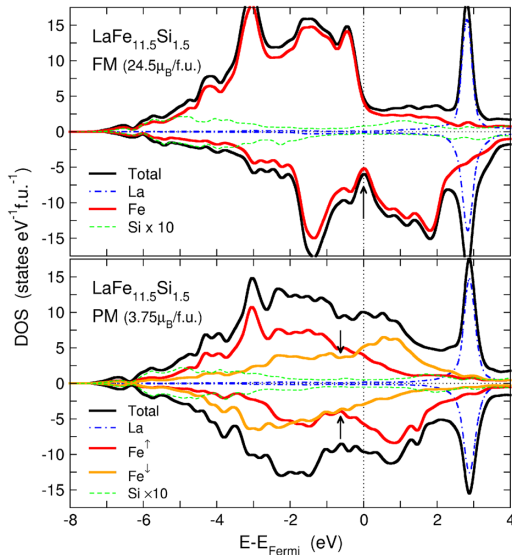
FIG. 4 (color online). Total and element-resolved electronic DOS of ferromagnetic ($M = 24.5\mu_B/\mathrm{f.u.}$, top) and paramagnetic ($M = 3.75\ \mu_B/\mathrm{f.u.}$, bottom) $\mathrm{LaFe_{11.5}Si_{1.5}}$ from DFT. The majority spin channel is denoted by positive values, the minority channel by negative values. The arrows mark the position of the pronounced mid-d-band minority spin pseudogap in the FM phase (top), and in the PM phase (bottom) its smeared-out and shifted remainders in the partial Fe DOS (denoted $\mathrm{Fe}^{\uparrow}$ and $\mathrm{Fe}^{\downarrow}$ according to the orientation of the Fe moments).

the FM phase. La and Si states are essentially absent in this important energy range. As is typical for an IEM, changing magnetic order (lower panel) distorts the minority Fe DOS ($\mathrm{Fe}^{\uparrow}$ and $\mathrm{Fe}^{\downarrow}$, for both magnetization directions, respectively) as states hybridize with the majority channel of neighboring antiparallel Fe. The local magnetic moment, i.e., the exchange splitting, at each site decreases, which shifts the features of the respective minority Fe DOS to lower energies including the remainders of the minimum. This suggests that magnetic disorder in La-Fe-Si affects restoring forces in a similar fashion as chemical ordering in FeV [84]. This also changes the Sommerfeld constant for the electronic specific heat by a factor of 2 ($\gamma_{\mathrm{PM}} = 56.1\ \mathrm{mJ\,kg^{-1}\,K^{-2}}$ versus $\gamma_{\mathrm{FM}} = 28.8\ \mathrm{mJ\,kg^{-1}\,K^{-2}}$), leading to the cooperative contribution of the electronic subsystem to the phase transition (cf. Fig. 2), similar to metamagnetic α-FeRh [85].

We conclude that in La-Fe-Si magnetic disorder causes unique changes in the VDOS. The consequence are significant cooperative contributions of magnetism, lattice, and electrons to the entropy change, which provide the foundation for the excellent magneto- and barocaloric properties of this compound. The electronic DOS minimum at E_F in the FM phase in combination with the itinerant nature of Fe magnetism is responsible for the anomalous magneto-elastic softening and the magnitude of ΔS_{lat} and ΔS_{el}. Both favor low-volume, low-moment configurations contributing to the Invar-type (over)compensation of

thermal expansion in the FM phase and foster an early, first-order-type transformation to the magnetically disordered phase. However, since our results indicate a strong interaction of all relevant degrees of freedom (i.e., electronic, vibrational, and magnetic), the common decomposition of ΔS_{iso} into three independent entropy terms must be interpreted with caution.

La-Fe-Si thus provides an ideal model system to unravel the contributions to magnetocaloric and Invar effect. Combining large-scale first-principles calculations and state-of-the-art scattering techniques provides the essential step to identify the microscopic mechanisms. As for other ferrous systems, NRIXS has proven to be an ideal experimental method to determine the specific vibrational contribution to the entropy change. In turn, we see the approximate modeling of structural and magnetic disorder in the 28 atom pseudo-ordered primitive cell, which grants us access to the electronic scale, justified by the excellent agreement in the VDOS of the Fe atoms. This approach thus provides a suitable basis for the exploration of improved materials and compositions. Our work suggests that maximizing the Fe content is the primary strategy to improve the magnetocaloric performance of the material, if the band filling is adjusted carefully by additional components.

[1] A. M. Tishin and Y. I. Spichkin, *The Magnetocaloric Effect and Its Applications*, Series in Condensed Matter Physics (Institute of Physics, Bristol, 2003).
[2] K. A. Gschneidner, Jr., V. K. Pecharsky, and A. O. Tsokol, Rep. Prog. Phys. **68**, 1479 (2005).
[3] O. Gutfleisch, M. A. Willard, E. Brück, C. H. Chen, S. G. Sankar, and J. P. Liu, Adv. Mater. **23**, 821 (2011).
[4] S. Fähler, U. K. Rößler, O. Kastner, J. Eckert, G. Eggeler, H. Emmerich, P. Entel, S. Müller, E. Quandt, and K. Albe, Adv. Eng. Mater. **14**, 10 (2012).

[5] V. K. Pecharsky and K. A. Gschneidner, Phys. Rev. Lett. **78**, 4494 (1997).

[6] K. G. Sandeman, Scr. Mater. **67**, 566 (2012).

[7] S. Fujieda, A. Fujita, and K. Fukamichi, Appl. Phys. Lett. **81**, 1276 (2002).

[8] J. Lyubina, R. Schäfer, N. Martin, L. Schultz, and O. Gutfleisch, Adv. Mater. **22**, 3735 (2010).

[9] J. Liu, M. Krautz, K. Skokov, T. G. Woodcock, and O. Gutfleisch, Acta Mater. **59**, 3602 (2011).

[10] H. Chang, J. Linag, B.-G. Shen, L.-T. Yang, F. Wang, N.-X. Chen, and G.-H. Rao, J. Phys. D **36**, 160 (2003).

[11] H. H. Hamdeh, H. Al-Ghanem, W. M. Hikal, S. M. Taher, J. C. Ho, D. T. K. Anh, N. P. Thuy, N. H. Duc, and P. D. Thang, J. Magn. Magn. Mater. **269**, 404 (2004).

[12] M. Rosca, M. Balli, D. Fruchard, D. Gignoux, E. K. Hlil, S. Miraglia, B. Ouladdiaf, and P. Wolfers, J. Alloys Compd. **490**, 50 (2010).

[13] T. Palstra, J. Mydosh, G. Nieuwenhuys, A. van der Kraan, and K. Buschow, J. Magn. Magn. Mater. **36**, 290 (1983).

[14] L. Jia, G. J. Liu, J. R. Sun, H. W. Zhang, and F. X. Hu, J. Appl. Phys. **100**, 123904 (2006).

[15] A. Fujita, S. Fujieda, Y. Hasegawa, and K. Fukamichi, Phys. Rev. B **67**, 104416 (2003).

[16] F. Wang, Y. F. Chen, G. J. Wang, J. R. Sun, and B. G. Shen, Chin. Phys. **12**, 911 (2003).

[17] A. Barcza, M. Katter, V. Zellmann, S. Russek, S. Jacobs, and C. Zimm, IEEE Trans. Magn. **47**, 3391 (2011).

[18] M. Krautz, K. Skokov, T. Gottschall, C. S. Teixeira, A. Waske, J. Liu, L. Schultz, and O. Gutfleisch, J. Alloys Compd. **598**, 27 (2014).

[19] F.-x. Hu, B.-g. Shen, J.-r. Sun, Z.-h. Cheng, G.-h. Rao, and X.-x. Zhang, Appl. Phys. Lett. **78**, 3675 (2001).

[20] L. Mañosa, D. Gonzáles-Alonso, A. Planes, M. Barrio, J.-L. Tamarit, I. S. Titov, M. Acet, A. Bhattacharyya, and S. Majumdar, Nat. Commun. **2**, 595 (2011).

[21] R. Huang, Y. Liu, W. Fan, J. Tan, F. Xiao, L. Qian, and L. Li, J. Am. Chem. Soc. **135**, 11469 (2013).

[22] E. F. Wassermann, in *Ferromagnetic Materials*, edited by K. H. J. Buschow and E. P. Wohlfahrt (Elsevier, Amsterdam, 1990), Vol. 5, Chap. 3, p. 237.

[23] A. Fujita and K. Fukamichi, IEEE Trans. Magn. **35**, 3796 (1999).

[24] A. Fujita, S. Fujieda, K. Fukamichi, H. Mitamura, and T. Goto, Phys. Rev. B **65**, 014410 (2001).

[25] A. Fujita, K. Fukamichi, J.-T. Wang, and Y. Kawazoe, Phys. Rev. B **68**, 104431 (2003).

[26] H. Yamada and T. Goto, Phys. Rev. B **68**, 184417 (2003).

[27] M. D. Kuz'min and M. Richter, Phys. Rev. B **76**, 092401 (2007).

[28] A. Fujita and H. Yako, Scr. Mater. **67**, 578 (2012).

[29] Z. Gercsi, K. G. Sandeman, and A. Fujita, arXiv:1407.7975.

[30] P. Entel, E. Hoffmann, P. Mohn, K. Schwarz, and V. L. Moruzzi, Phys. Rev. B **47**, 8706 (1993).

[31] G.-J. Wang, F. Wang, N.-L. Di, B.-G. Shen, and Z.-H. Cheng, J. Magn. Magn. Mater. **303**, 84 (2006).

[32] M.-K. Han and G. J. Miller, Inorg. Chem. **47**, 515 (2008).

[33] A. Boutahar, E. K. Hlil, H. Lassri, and D. Fruchart, J. Magn. Magn. Mater. **347**, 161 (2013).

[34] T. Mukherjee, S. Michalski, R. Skomski, D. J. Sellmyer, and C. Binek, Phys. Rev. B **83**, 214413 (2011).

[35] P. J. von Ranke, N. A. de Oliveira, C. Mello, A. M. G. Carvalho, and S. Gama, Phys. Rev. B **71**, 054410 (2005).

[36] See Supplemental Material at http://link.aps.org/supplemental/10.1103/PhysRevLett.114.057202, which includes Refs. [37–64], for supporting information on first-principles modeling, experimental details and thermodynamic analysis.

[37] P. Hohenberg and W. Kohn, Phys. Rev. **136**, B864 (1964).

[38] M. E. Gruner and P. Entel, J. Phys. Condens. Matter **21**, 293201 (2009).

[39] J. P. Perdew, K. Burke, and Y. Wang, Phys. Rev. B **54**, 16533 (1996).

[40] S. H. Vosko, L. Wilk, and M. Nusair, Can. J. Phys. **58**, 1200 (1980).

[41] J. P. Perdew, K. Burke, and M. Ernzerhof, Phys. Rev. Lett. **77**, 3865 (1996).

[42] M. E. Gruner and P. Entel, Phys. Rev. B **83**, 214415 (2011).

[43] M. Methfessel and A. T. Paxton, Phys. Rev. B **40**, 3616 (1989).

[44] P. E. Blöchl, O. Jepsen, and O. K. Andersen, Phys. Rev. B **49**, 16223 (1994).

[45] V. L. Moruzzi, P. M. Marcus, K. Schwarz, and P. Mohn, Phys. Rev. B **34**, 1784 (1986).

[46] G. Kresse, J. Furthmüller, and J. Hafner, Europhys. Lett. **32**, 729 (1995).

[47] X. Gonze and C. Lee, Phys. Rev. B **55**, 10355 (1997).

[48] K. Parlinski, Z.-Q. Li, and Y. Kawazoe, Phys. Rev. Lett. **78**, 4063 (1997).

[49] M. A. Uijttewaal, T. Hickel, J. Neugebauer, M. E. Gruner, and P. Entel, Phys. Rev. Lett. **102**, 035702 (2009).

[50] S. Ener, J. Neuhaus, W. Petry, R. Mole, K. Hradil, M. Siewert, M. E. Gruner, P. Entel, I. Titov, and M. Acet, Phys. Rev. B **86**, 144305 (2012).

[51] K. S. Singwi and A. Sjölander, Phys. Rev. **120**, 1093 (1960).

[52] W. Sturhahn and V. G. Kohn, Hyperfine Interact. **123/124**, 367 (1999).

[53] A. I. Chumakov and W. Sturhahn, Hyperfine Interact. **123/124**, 781 (1999).

[54] M. Hu, W. Sturhahn, T. Toellner, P. Hession, J. Sutter, and E. E. Alp, Nucl. Instrum. Methods Phys. Res., Sect. A **428**, 551 (1999).

[55] M. Y. Hu, T. S. Toellner, N. Dauphas, E. E. Alp, and J. Zhao, Phys. Rev. B **87**, 064301 (2013).

[56] S. Stankov, Y. Z. Yue, M. Miglierini, B. Sepiol, I. Sergueev, A. I. Chumakov, L. Hu, P. Svec, and R. Rüffer, Phys. Rev. Lett. **100**, 235503 (2008).

[57] M. Kresch, Ph.D. thesis, California Institute of Technology, 2009.

[58] R. Bozorth, *Ferromagnetism* (van Nostrand, New York, 1951).

[59] H. Hasegawa, M. W. Finnis, and D. G. Pettifor, J. Phys. F **15**, 19 (1985).

[60] R. Boehler and J. Ramakrishnan, J. Geophys. Res. **85**, 6996 (1980).

[61] M. Lucas, J. Muñoz, O. Delaire, N. Markovskiy, M. Stone, D. Abernathy, I. Halevy, L. Mauger, J. Keith, M. Winterrose *et al.*, Phys. Rev. B **82**, 144306 (2010).

[62] C. Wolverton and A. Zunger, Phys. Rev. B **52**, 8813 (1995).

[63] A. F. Guillermet and G. Grimvall, Phys. Rev. B **40**, 1521 (1989).

[64] R. Lübbers, H. F. Grünsteudel, A. I. Chumakov, and G. Wortmann, Science **287**, 1250 (2000).

[65] M. Seto, Y. Yoda, S. Kikuta, X. W. Zhang, and M. Ando, Phys. Rev. Lett. **74**, 3828 (1995).

[66] W. Sturhahn, T. S. Toellner, E. E. Alp, X. W. Zhang, M. Ando, Y. Yoda, S. Kikuta, M. Seto, C. W. Kimball, and B. Dabrowski, Phys. Rev. Lett. **74**, 3832 (1995).

[67] A. I. Chumakov, R. Rüffer, H. Grünsteudel, H. F. Grünsteudel, G. Grübel, J. Metge, O. Leupold, and H. A. Goodwin, Europhys. Lett. **30**, 427 (1995).

[68] T. S. Toellner, Hyperfine Interact. **125**, 3 (2000).

[69] W. Sturhahn, Hyperfine Interact. **125**, 149 (2000).

[70] G. Kresse and J. Furthmüller, Phys. Rev. B **54**, 11169 (1996).

[71] G. Kresse and D. Joubert, Phys. Rev. B **59**, 1758 (1999).

[72] J. P. Perdew, in *Electronic Structure of Solids '91*, edited by P. Ziesche and H. Eschrig (Akademie Verlag, Berlin, 1991).

[73] F. Wang, G.-J. Wang, F.-X. Hu, A. Kurbakov, B.-G. Shen, and Z.-H. Cheng, J. Phys. Condens. Matter **15**, 5269 (2003).

[74] D. Alfè, Comput. Phys. Commun. **180**, 2622 (2009).

[75] G. Grimvall, *Thermophysical Properties of Materials*, Selected Topics in Solid State Physics Vol. 18 (North-Holland, Amsterdam, 1986).

[76] B. Fultz, Prog. Mater. Sci. **55**, 247 (2010).

[77] J. Neuhaus, M. Leitner, K. Nicolaus, W. Petry, B. Hennion, and A. Hiess, Phys. Rev. B **89**, 184302 (2014).

[78] V. V. Struzhkin, H.-k. Mao, J. Hu, M. Schwoerer-Böhning, J. Shu, R. J. Hemley, W. Sturhahn, M. Y. Hu, E. E. Alp, P. Eng, and G. Shen, Phys. Rev. Lett. **87**, 255501 (2001).

[79] J. Rosén and G. Grimvall, Phys. Rev. B **27**, 7199 (1983).

[80] O. Eriksson, J. M. Wills, and D. Wallace, Phys. Rev. B **46**, 5221 (1992).

[81] X. Liu, Z. Altounian, and D. Ryan, J. Phys. Condens. Matter **15**, 7385 (2003).

[82] O. Delaire, M. S. Lucas, J. A. Muñoz, M. Kresch, and B. Fultz, Phys. Rev. Lett. **101**, 105504 (2008).

[83] O. Delaire, K. Marty, M. B. Stone, P. R. C. Kent, M. S. Lucas, D. L. Abernathy, D. Mandrus, and B. C. Sales, Proc. Natl. Acad. Sci. U.S.A. **108**, 4725 (2011).

[84] J. Muñoz, M. Lucas, O. Delaire, M. Winterrose, L. Mauger, C. Li, A. Sheets, M. Stone, D. Abernathy, Y. Xiao *et al.*, Phys. Rev. Lett. **107**, 115501 (2011).

[85] A. Deák, E. Simon, L. Balogh, L. Szunyogh, M. dos Santos Dias, and J. B. Staunton, Phys. Rev. B **89**, 224401 (2014).